Synthetic Metals 217 (2016) 220–230

Contents lists available at ScienceDirect

Synthetic Metals

journal homepage: www.elsevier.com/locate/synmet

Polyaniline/Graphene nanocomposite coatings on copper: Electropolymerization, characterization, and evaluation of corrosion protection performance

Y. Jafari, S.M. Ghoreishi*, M. Shabani-Nooshabadi

Department of Analytical Chemistry, Faculty of Chemistry, University of Kashan, Kashan, Islamic Republic of Iran

ARTICLE INFO

Article history:
Received 30 November 2015
Received in revised form 16 March 2016
Accepted 4 April 2016
Available online xxx

Keywords:
Copper
Electropolymerization
EIS
Graphene
Corrosion

ABSTRACT

Polyaniline–graphene nanocomposite film was electrochemically deposited by cyclic voltammetry on copper electrode. The corrosion resistance of polyaniline–graphene nanocomposite covered copper substrates was estimated using potentiodynamic polarization and electrochemical impedance spectroscopy techniques in 5000 ppm NaCl aqueous solution at room temperature. Potentiodynamic Polarization results show that corrosion potentials shift to anodic regions in the presence of polyaniline–graphene nanocomposite compared to the blank solution. The electrochemical measurements, also, indicated that the inhibition efficiency for polyaniline-graphene nanocomposite is 98%.

1. Introduction

Copper has been one of the important materials in the industry owing to its high electrical and thermal conductivity, mechanical workability, and its relatively noble properties. It is widely used in many applications of electronic industries and communications as a conductor; also, it is used in electrical power lines, pipelines for domestic and industrial water utilities, heat conductors, and heat exchangers. Thus, corrosion of copper and improving the corrosion resistance of this metal in a wide variety of media has attracted the attention of researchers [1–5].

In order to protect metal surfaces, use of conducting polymers as advanced coating materials has become one of the most exciting research fields in recent decades [6–8]. Therefore, the goals of synthesizing these coatings as in metals and evaluating their corrosion protection properties have led to growing interest.

A common method involves the application of protective coatings made from paints, organic resins, plastics, or films of noble metals on the structure itself (e.g., the coating on tin cans) [9]. These coatings form an impervious barrier between the metal and the oxidant but are only effective when the coating completely covers the structure. Flaws in the coating have been found to produce accelerated corrosion of the metal. Within coating technology, there is increasing interest in the development of an efficient anticorrosive coating that is able to replace the conventional inorganic anticorrosive pigments usually added to paints, which may have detrimental effects on both environment and health. Researchers have invented a revolutionary corrosion control system using conducting polymers in the last two decades [10]. Since DeBerry [11] reported that an electrochemically deposited polyaniline film could provide anodic protection for stainless steel, conductive polymers have been candidates for metal protection against corrosion [12–15]. Polyaniline is one of the most extensively investigated conducting polymers because of its good stability, low cost, low toxicity and valuable electronic properties.

Polyaniline exhibit different chemical structures that are both pH and potential dependent [16]: leucoemeraldine base (LB: fully reduced form), leucoemeraldine salt (LS: fully reduced and protonated form), emeraldine base (EB: half-oxidized form), emeraldine salt (ES: half-oxidized and protonated form) and pernigraniline base (PB: fully oxidized form). The emeraldine form has excellent air and thermal stability [17] and thus has been extensively studied for corrosion control either as a thin primer, pigment or coating on inorganic pigment. Anticorrosive effect of polyaniline has been explored for aluminum and aluminum alloys [18,19], mild steel [20], stainless steel [21,22], iron [23,24], copper [25] and other metals [26,27].

Recent investigations have shown that the synthesis of polymers in the presence of nanoparticles can increase the

* Corresponding author.
E-mail address: s.m.ghoreishi@kashanu.ac.ir (S.M. Ghoreishi).

http://dx.doi.org/10.1016/j.synthmet.2016.04.001
0379-6779/

polymer surface area [28]. Over the last decade, nano-sized fillers have played an important role in improving the corrosion resistance and the thermal and mechanical properties of the coatings. Organic coatings have been employed to protect steel surfaces against mobile corrosion environments for a long time by introducing a barrier to prohibit ionic transport and electrical conduction. There are various reports about the improvement of coatings performance in such environments using nanoparticles as reinforcement such as TiO_2 [29,30], SiO_2 [31], ZnO [32], Fe_2O_3 [33], carbon nanotube [34,35] and graphene [36].

Graphene, which is a two-dimensional monolayer of sp^2 bonded carbon, has been attracting increasing scientific and technological attention due to its outstanding mechanical, optical, thermal and electrical properties [37,38]. Graphene exhibits potential application in many fields such as sensors [39,40], nano-electronics [41], electrode materials for electrochemical capacitors and lithium ion batteries [42]. Wide studies have been devoted to graphene preparation, reduction of graphene oxide and the synthesis and application of graphene-based composites [43–45].

Recently, graphene, one of the most compelling materials, has been reported to be an excellent anticorrosion material because it possesses many unique characteristics that are ideal for anticorrosion, such as chemical inertness, excellent thermal and chemical stability, remarkable flexibility, and impermeable to molecules. Chang et al. [46] presented the application of polymer/graphene composites for the anti-corrosion of steel. The coating was able to effectively protection steel because of its good impermeability to O_2 and H_2O. Yu et al. [47] successfully prepared well-dispersed polystyrene/modified graphene oxide composites by in situ mini-emulsion polymerization and used it for corrosion protection. The as-prepared composites exhibited superior anticorrosion properties compared with pure polystyrene. Singh et al. [48] reported a robust graphene reinforced composite coating with an excellent anticorrosion performance by cathodic electrophoretic deposition. They believed that cathodic electrophoretic deposition was more advantageous than CVD on producing a coating of controlled microstructure on a wide range of substrates.

However, research investigating graphene-based polymer nanocomposites for corrosion protection is scant. For example, Compton et al. [49] found that polystyrene film with a low graphene loading was superior in reducing the relative O_2 permeability of polystyrene compared with those of the best published gas barrier results for polymer/clay composites.

In the work reported in this paper, we have made an attempt to synthesize adherent polyaniline/graphene (PANI/G) nanocomposite coatings on Copper (Cu) substrates by cyclic voltammetry method from aqueous sodium salicylate solution and examined the ability of these coatings to serve as corrosion protective coatings on Cu. To the best of our knowledge, there are no reports in the literature dealing with the direct deposit of PANI/G nanocomposite coatings on Cu from aqueous solution. The objectives of the present study are: (a) to find an appropriate current density, low cost and easily available electrolyte for the electrochemical synthesis of PANI/G nanocomposite coating on Cu substrates; (b) to characterize these coatings by using spectroscopic techniques and (c) to examine the possibility of utilizing the PANI/G nanocomposite coatings for corrosion protection of Cu in aqueous 5000 ppm NaCl solution.

2. Experimental

2.1. Materials

Aniline (99%), sodium salicylate (99%) and sodium dodecyl sulfate (SDS) were purchased from Merck. All the analytical grade chemicals were used as received. Graphene was obtained from the Chinese Academy of Sciences and had outside diameters of 10–20 nm and purities of over 95%. Aqueous electrolytes used for the synthesis of the nanocomposite were prepared using double distilled water. All experiments were carried out at room temperature. The graphene (0.1 g) was ultra-sonicated for 1 h in 10 mL double distilled water. SDS was used as a surfactant to disperse graphene in water since this prevents them from becoming aggregated for a long period.

As a typical procedure for the preparation of PANI/G nanocomposite coatings with 0.01 wt% of graphene, then, a mixture of 0.4 M of sodium salicylate and 0.2 M of aniline monomer was added into the graphene solution under magnetic stirring for 1 h. Subsequently, the obtained solution was ultrasonicated for 20 min in order to increase its uniformity.

2.2. Instrumentation

SAMA potentiostat/galvanostat system was used for electropolymerization and also, AUTOLAB PGSTAT 30 (Eco Chemie, Utrecht the Netherlands) potentiostat/galvanostat system was used for corrosion studies. This system was interfaced to a personal computer to control the experiments, and the data were analyzed using NOVA 1.6 software. The structure of PANI/G nanocomposite film on the Cu surface was analyzed by FTIR spectrophotometry (Perkin-Elmer, Spectrum One, with universal ATR attachment with a diamond and ZnSe crystal) and the electropolymerized PANI/G nanocomposite was dissolved in pure *n*-methylpyrrolidone (NMP). A UV–vis spectrum of this polymer solution was recorded on a PERKIN ELMER Lambda2S UV–vis spectrometer. The XRD patterns were recorded by a Rigaku D-max CIII X-ray diffractometer using Ni-filtered Cu Kα radiation. Morphologies of PANI/G nanocomposite coated Cu surfaces were investigated via a field-emission scanning electron microscope (Hitachi FE-SEM S4800). The analysis of the impedance spectra and fitting of the experimental results to equivalent circuits were performed by using NOVA 1.6 software from Princeton Applied Research.

2.3. Electropolymerization process and corrosion tests

Electropolymerization was carried out by cyclic voltammetry from 10 mL of the prepared solution at pH 12.5 [50]. After the electropolymerization reaction, the green colored, homogeneous and adherent PANI/G nanocomposite coatings were successfully obtained on the Cu surface. Electropolymerization and subsequent electrochemical studies (stability and corrosion tests) were carried out in single compartment three electrode cell, consisting of Cu (99% purity) sheet as a working electrode, platinum wire as the counter electrode (CHI Instruments), and Ag/AgCl (3 M KCl) as the reference electrode. The metal sheet was cut into rectangular samples of 1 cm^2 area soldered with Cu-wire for an electrical connection. The metal sheet then mounted onto the epoxy resin to offer only one active flat surface exposed to the corrosive environment. Before each test, the steel surface was abraded with a 2000 grit emery paper then washed with distilled water and used for electropolymerization.

PANI/G nanocomposite coatings were electrochemically synthesized by cyclic voltammetry (CV) with the working electrode potential between −1.5 and 1.8 V at scan rate 0.05 V/s by applying 10 cycles.

Corrosion tests of uncoated and PANI/G nanocomposite coated Cu electrode was carried out in aerated 5000 ppm NaCl solution, at room temperature by electrochemical impedance spectroscopy (EIS) and polarization techniques. All impedance and polarization curves were recorded at open circuit potential, in an unstirred state, after 120 min of immersion of the electrode in the corrosive

test solution, and the time to reach a stable open circuit potential was limited to 120 min due to the fact that surface conditions may be altered within a longer period. In the case of Tafel polarization, the potential was scanned at ±200 mV versus OCP at a scan rate of 0.001 V s^{-1}. From the anodic and cathodic polarization curves, the Tafel regions were identified and extrapolated to the corrosion potential (E_{corr}) to obtain the corrosion current density (I_{corr}) using the NOVA 1.6 software. In the case of electrochemical impedance spectroscopy, a.c. signals of 10 mV amplitude and various frequencies from 100 kHz to 0.01 Hz at open circuit potentials were impressed to the coated Cu in the electrode surface (1 cm^2). A Pentium IV powered computer and NOVA 1.6 software was applied for analyzing impedance data.

3. RESULTS and DISCUSSION

3.1. Electrosynthesis of PANI/G nanocomposite

Fig. 1 shows the CV of the 10 cycles in 0.4 M sodium salicylate solution containing 0.2 M aniline and 0.01%w/w dispersed graphene. In the first anodic potential scan, the irreversible oxidation peak starting from about + 0.7 V corresponds to aniline oxidation and this oxidation process gives a start to the formation of the PANI film on the Cu surface [51]. The positive cycle of these voltammograms is characterized by: an anodic peak at the +0.7 V which has been attributed to the transformation of PANI from reduced leucoemeraldine (LE) state to the partially oxidized emeraldine (EM) and the conversion of emeraldine to fully oxidized pernigraniline (PF)form. This behavior can be explained

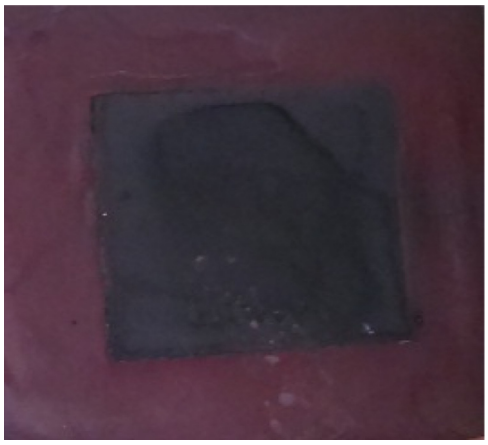

Fig. 2. Image of formation of the black layer PANI/G nanocomposite in the substrate Cu.

in the following mode: it is well known that PANI/G nanocomposite can exist in three different oxidation states, such as leucoemeraldine (fully reduced form), emeraldine (partially oxidized form) and pernigraniline (fully oxidized form). These forms of PANI/G nanocomposite are dependent on the applied potential. The reduction peak at −0.9 V is due to the transformation of PANI/G from emeraldine to leucoemeraldine state. Increases in the current of peak shows that the deposition thickness increases with cycles [1,52–57].

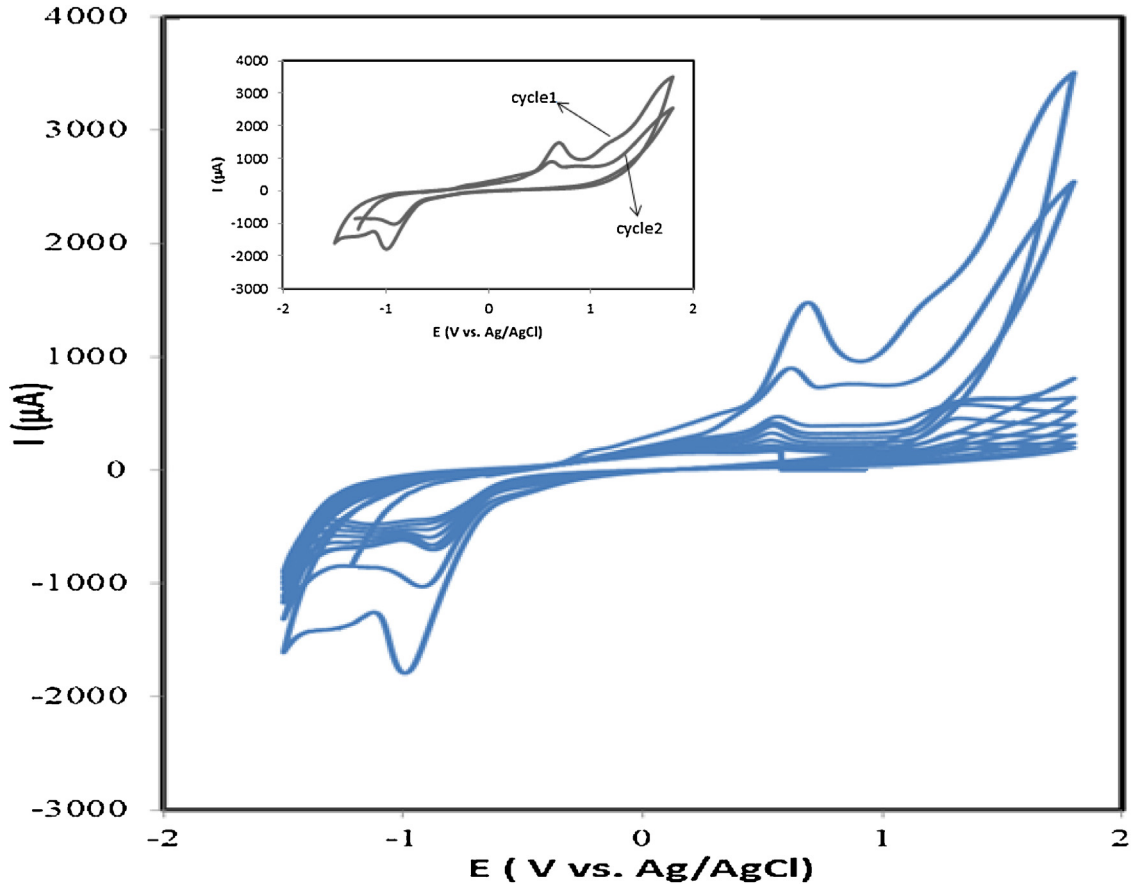

Fig. 1. CV curves of pure PANI/G nanocomposite coating during continuous voltammograms in a solution of 0.2 M of aniline in 0.4 M of sodium salicylate with 0.01% w/w graphene at 50 mV/s.

It is clearly seen that the position of peak +0.7 V is shifted in anodic direction and the current density corresponding to this peak decreases gradually with the number of scans. At the end of 10 cycles, a dark green colored, uniform PANI/G film was synthesized on the Cu surface (Fig. 2). In order to examine the adhesion of the PANI/G nanocomposite coating over Cu substrates, the ASTM D 3359 standard tape adhesion test was applied and the adhesion remaining (AR%) values of all the coatings exhibited above 95% without any failed regions, 5B, which implies good adhesive strength of PANI/G nanocomposite coating toward Cu surface [58].

3.2. Characterization of nanocomposite coating

3.2.1. Electrochemical measurement

Cyclic voltammogram of PANI/G nanocomposite, deposited on a Cu electrode, was recorded in an aqueous solution of 0.5 M sodium salicylate solution has shown in Fig. 3. CV of PANI/G nanocomposite exhibit one pairs of redox waves with the first one observed at E = 0.6 V indicating the transformation of leucoemeraldine from to conducting emeraldine form and the second one at E = 1.2 V which is due to the conversion of emeraldine into the pernigraniline form. A pair of humps in the region of E = −1 V has been assigned to overoxidation products. This indicates that graphene layer influenced the electrochemical properties of polyaniline the intercalation favor a polymer with different properties as could evidence with this electrochemical technique. There is only a minor shift of the reduction peak associated with the pernigraniline-emeraldine transition [59].

3.2.2. Spectroscopic characterization

Fig. 4 shows the UV–vis spectrum of graphene, PANI and PANI/G nanocomposite film. The characteristic peaks of the PANI/G nanocomposite doped by sodium salicylate appeared at 350 and 650 nm, which was attributed to polaron-π^* and π-polaron transitions, respectively [60]. The spectrum of PANI/G nanocomposite film was similar to that of the polyaniline [50], except that the absorbance intensity of the former was lower than that of the latter. In addition, the absorption peaks of the π-polaron transition of the two were broader and appeared at the high wavelength. This result indicated that the polyaniline of the two samples with high doping level was delocalized.

Fig. 5 show the FTIR spectrum of graphene (a), polyaniline (b) and the PANI/G nanocomposite (c) film. The presence of the graphene sheets can be confirmed by the FTIR data, as shown in Fig. 5. The FTIR spectrum of graphene shows a strong absorption band at 1620 cm^{-1} due to aromatic C=C as well as bands due to carboxy C—O 1420 cm^{-1} groups situate at the edges of the graphene nanosheets while the broadband at ca. 3300 cm^{-1} can be due to the O—H stretching mode. This is in agreement with the reported data [61,62]. However, these absorption bands are decreased significantly in the FTIR spectrum of the PANI/G nanocomposite film, indicating that most of the functional groups have been essentially removed by electrochemical reduction. As shown in Fig. 5, the main peaks at 1570 and 1460 cm^{-1} can be assigned to the stretching vibrations of quinoid and benzene rings, respectively. The peaks at 1292 and 1227 cm^{-1} correspond to the C—N stretching vibration. The in-plane bending of C—H is reflected in the 1111 cm^{-1} peak. The peak at 790 cm^{-1} is attributed to the out-of-plane bending of C—H. All of the above peaks can be seen from a spectrum of PANI/G nanocomposite film, showing graphene is existent in the nanocomposite film [57].

3.2.3. XRD analysis

The crystal structure of PANI/G nanocomposites was characterized by X-ray diffraction (XRD). The XRD pattern of PANI/G nanocomposites is shown in Fig. 6. The XRD patterns of PANI/G nanocomposite coating regarded to in the emeraldine salt form. Polyaniline has basically pseudo-orthorhombic crystal structure with chains parallel to the c-axis where the dopant ions are present at the central of the cell. The XRD pattern of polyaniline shows a broad peak at around 35 θ. This reflection is indexed to the (1 1 0) plane and the ionomer decreases the order of the stacking formed by polyaniline chains and graphene. This could imply that the polyaniline on the surface of graphene sheet maintains a similar crystal structure to pure polyaniline [63].

3.2.4. Thermal gravimetric analysis

Fig. 7 depicts TGA thermogram in the air of neat polyaniline and PANI/G nanocomposite. The TGA curves show, as expected, that as graphene content adds the thermal stability of the composite is higher since graphene is significantly more stable than polyaniline. Furthermore, the addition of graphene also produces a char barrier effect that prevents oxygen from reaching the material and thus lowering the burning rate and increasing thermal stability [64,65].

3.3. Corrosion tests

3.3.1. Potentiodynamic polarization studies

Fig. 8 displays the typical potentiodynamic polarization curves obtained on uncoated and coated Cu substrates in 5000 ppm NaCl solution. The values of E_{corr}, I_{corr}, corrosion rate (CR) and

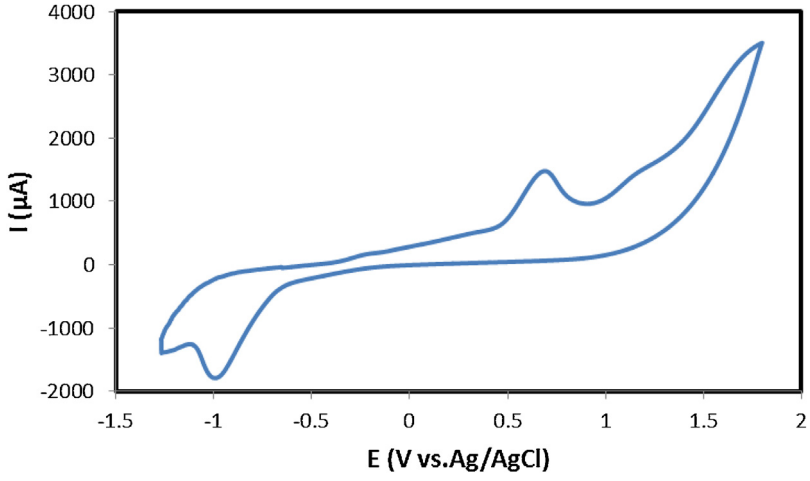

Fig. 3. CV curve for PANI/G nanocomposite coating on Cu substrates in 0.5 M sodium salicylate solution.

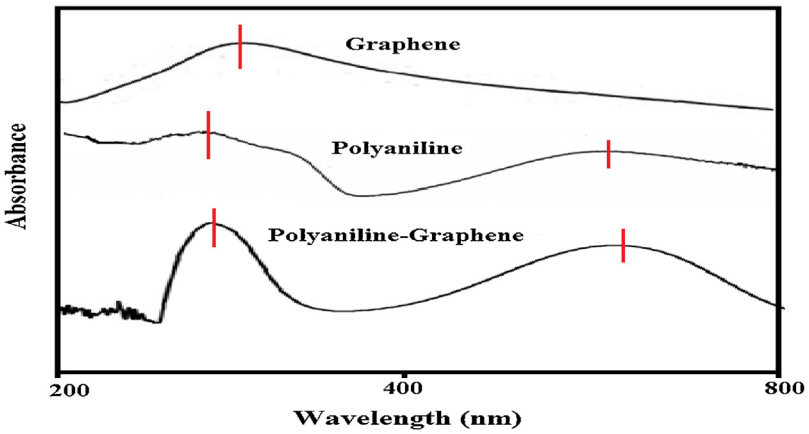

Fig. 4. UV–vis spectrum recorded for graphene, polyaniline and PANI/G nanocomposite electrosynthesized on the Cu.

polarization resistance (Rp) (calculated using NOVA software) are given in Table 1. Compared with the uncoated Cu substrate, all the coated Cu exhibited a drastic shift of corrosion potential (E_{corr}) in the anodic region thus revealing the improved corrosion resistance of the coated Cu substrates. It was also observed that both anodic and cathodic current densities reduced appreciably by at least one decade after the coating. In particular, after addition of graphene into polyaniline, the coated substrates exhibit much lower current density than that of pure polyaniline coated and uncoated Cu, demonstrating a reduction in the corrosion rate of the PANI/G nanocomposite coated substrates. Precisely, PANI/G nanocomposite coatings offer an enhanced corrosion protection for the Cu substrate under the free corrosion potential condition.

From the measured I_{corr} values, the protection efficiency (PE) was obtained from the following equation [50]:

$$PE = (I_{corr} - I_{corr(c)})/I_{corr} \times 100 \quad (1)$$

that I_{corr} and $I_{corr(c)}$ are the corrosion current density values in the absence and presence of the coating, respectively.

As it can be seen in Table 1, when the PE increases, I_{corr} decrease from 5.2 $\mu A\,cm^{-2}$ for uncoated Cu to 1.8 and 0.1 $\mu A\,cm^{-2}$ for polyaniline and PANI/G nanocomposite coated Cu under optimal condition respectively. From Table 1, it can be also found that the corrosion rate of Cu is significantly reduced as a result of the reduction in I_{corr}. The corrosion rate of the polyaniline and PANI/G nanocomposite coated Cu are found to be 4×10^{-3} and 9×10^{-5} mm $year^{-1}$, respectively, which are about 5 and 222 times lower than that observed for bare Cu.

The porosity in the coating strongly governs the anticorrosive behavior of the coatings; therefore, the determination of porosity in the coating is essential in order to estimate the overall corrosion resistance of the coated substrate. The porosity in PANI/G nanocomposite coatings on Cu substrates was determined from potentiodynamic polarization measurements. The porosity of the polymer coatings were calculated using the following equation [66]:

$$P = (R_{puc}/R_{pc}) \times 10^{-(|DE|/b_a)} \quad (2)$$

where P is the total porosity, R_{puc} and R_{pc} are the polarization resistance of the uncoated and coated Cu, respectively. ΔE_{corr} is the difference between the corrosion potentials and b_a is the anodic Tafel slope for the uncoated Cu substrate. The calculated porosity value of the PANI/G nanocomposite coating is also given in Table 1. As seen in the tables, the P value of the coating decreases with an increase graphene in the polymer coatings. As a result, there is a

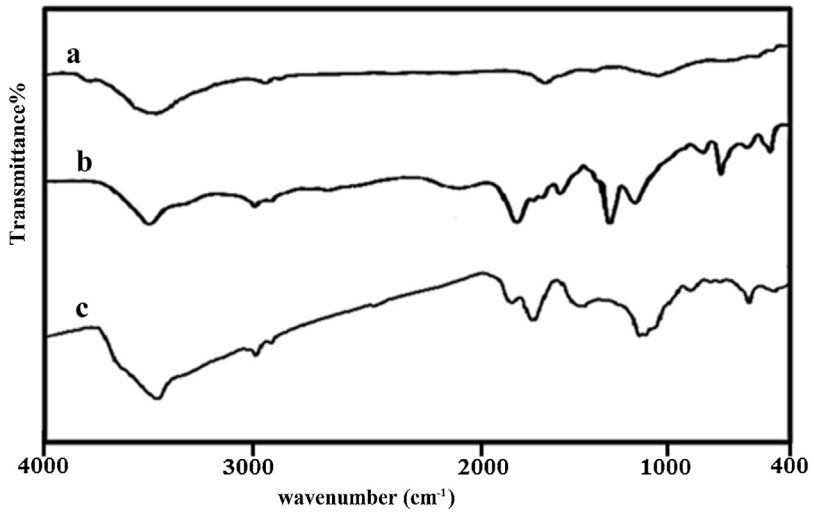

Fig. 5. FT-IR spectra (a) graphene nanoparticles, (b) polyaniline and (c) the PANI/G nanocomposite.

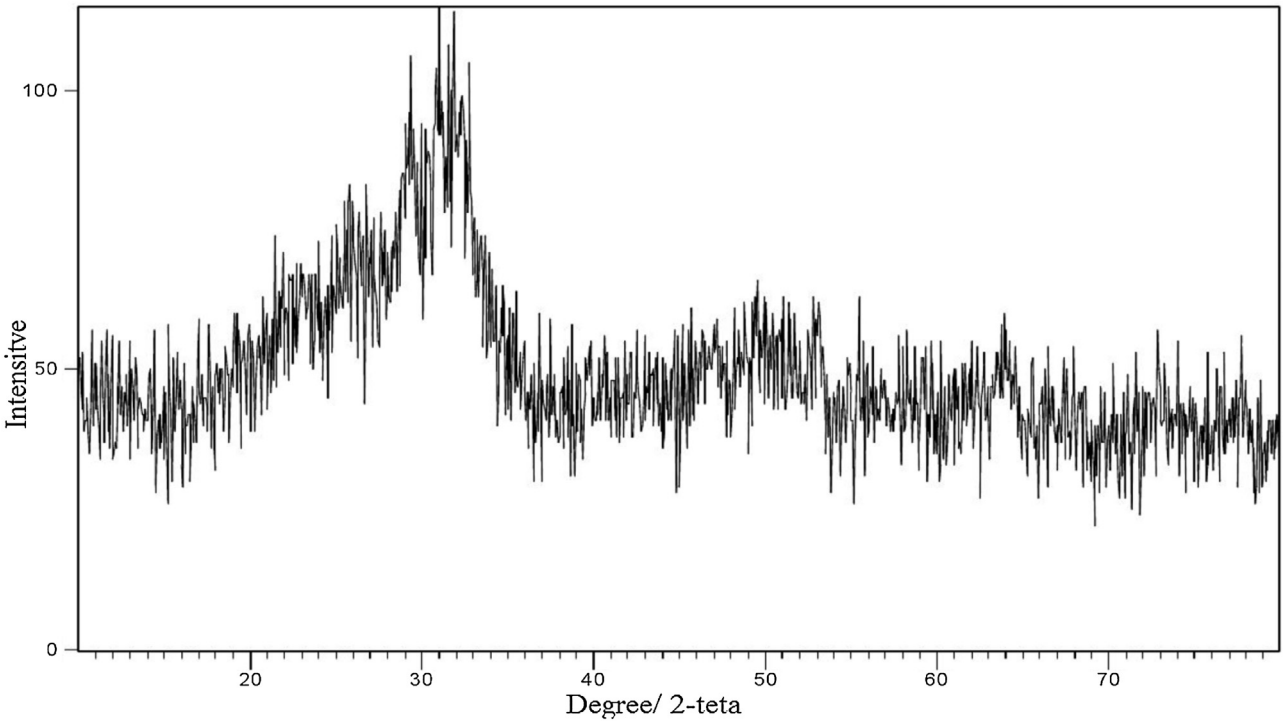

Fig. 6. X-ray diffraction pattern the PANI/G nanocomposite.

decrease in the accessibility of the aggressive species to the Cu surface and, therefore, a decrease occurs in the corrosion rate and corrosion current values. The lower values of the porosity in the PANI/G nanocomposite coatings permit an improvement of the corrosion resistance by hindering the access of the electrolyte to the Cu substrates.

The electrochemical parameters obtained from polarization curves are summarized in Table 1. From the obtained results, it could be seen that the PANI/G nanocomposite coating exhibited much-improved corrosion resistance property than the polyaniline coated and uncoated Cu substrates. It is well-known that a dense and compact polyaniline coating reinforced with graphene provides an improved protective barrier layer to diminish the corrosion of metal substrates, whereas porous polyaniline coatings might not offer such adequate protection as more electrolytic species can penetrate through the coating to the underlying

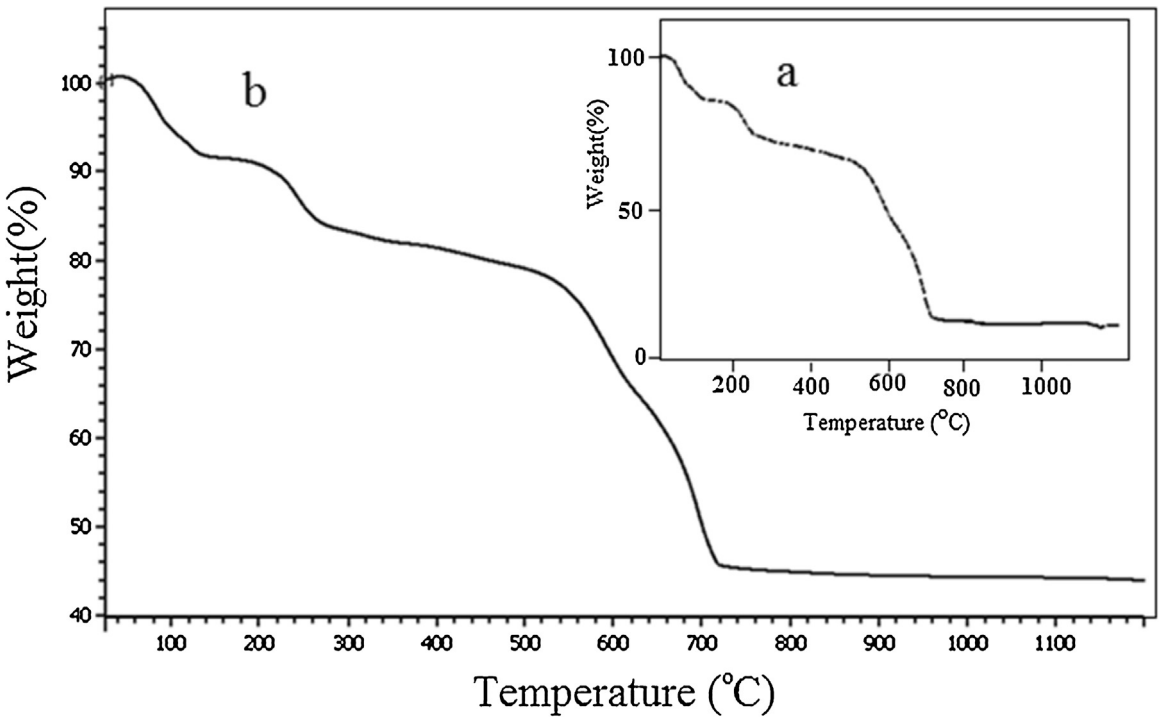

Fig. 7. Thermal gravimetric analysis of polyaniline and PANI/G nanocomposite with 0.01% w/w graphene.

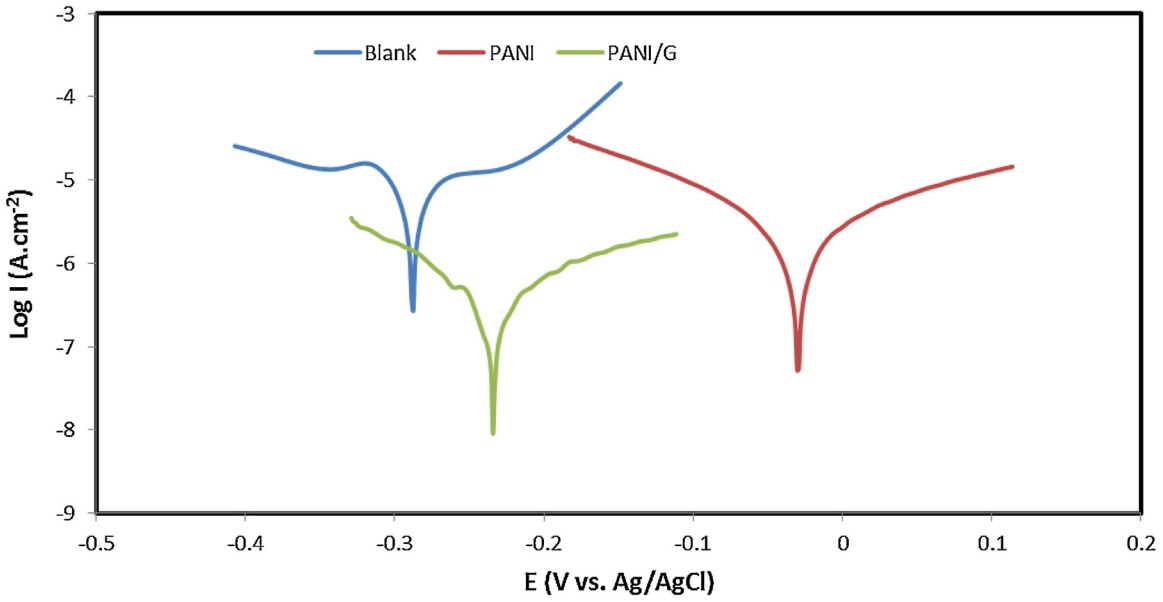

Fig. 8. Polarization behavior of electropolymerized PANI/G nanocomposite-coated on Cu in 5000 ppm NaCl solution.

substrate. A possible justification for the improved corrosion protection performance of PANI/G nanocomposite coating is provided by the hydrophobic surface and the higher interaction energies between the graphene and polyaniline [67].

3.3.2. EIS analysis

The Nyquist impedance plots of uncoated Cu and PANI/G nanocomposite coated Cu recorded in a 5000 ppm NaCl solution are shown in Fig. 9. The values of the impedance parameters of the best fit to the experimental impedance plots for uncoated Cu and PANI/G nanocomposite coated Cu with the equivalent circuits are given in Table 2 and with an error rate of less than 10%.

The equivalent circuit consists of the electrolyte resistance (R_s), the pore resistance (R_{por}) which is due to the formation of the ion conducting paths across the coating, the coating capacitance (Q_c), the charge transfer resistance (R_{ct}) of the area at the Cu coatings interface, where corrosion occurs and double layer capacitance (Q_{dl}) [51,68,69]. Instead of capacitance, a constant phase element (Q) was used. The Q represents the deviation from the true capacitance behavior. Q is a constant which represents the true capacitance of the oxide barrier layer. The Q (which represents a deviation from the true capacitor behavior) is used here instead of an ideal double layer capacitance. The impedance of Q with the value of n is often associated with a non-uniform current distribution due to the porous oxide layer. Q describes an ideal capacitor for n = 1, an ideal resistor for n = 0, and a pure inductor for n = −1 [70].

The percentage PE was calculated using the following equation [71]:

$$PE = \frac{R_{ct(c)} - R_{ct}}{R_{ct(c)}} \times 100 \quad (3)$$

where R_{ct} and $R_{ct(c)}$ are the charge transfer resistance in the absence and presence of coating, respectively. The R_{ct} value is approximately 90 and 118 kΩ cm^2 for polyaniline and PANI/G nanocomposite, respectively, which are about 2.7 and 3.5 times higher than that of uncoated Cu. The higher value of R_{ct} is attributed to the effective barrier behavior of the PANI/G nanocomposite coating. The lower values of C_{dl} for the PANI/G nanocomposite coated Cu provide further support for the protection of Cu by the PANI/G nanocomposite coating. Thus, the higher value of R_{ct} and lower value of C_{dl} indicate the excellent corrosion performance of the PANI/G nanocomposite coating. The PE% calculated from EIS data is found to be 63.3% and 72% for polyaniline and PANI/G nanocomposite, respectively, which is in agreement with the potentiodynamic polarization results. Increase in R_{ct} values of the PANI/G nanocomposite coated electrode may result from the catalytic effect of PANI/G nanocomposite coating that leads to the formation of the insoluble Cu sulfate layer [58].

One of the important parameters for the synthesis of the polymer coatings on the metal surface is calculating coating thickness which is an important feature for industrial applications. EIS data can be used for measurement of the thickness of PANI/G nanocomposite coating. The nanocomposite coating thickness on the surface of Cu by using of C_{dl} can be achieved according to the following equation [72]:

$$Q_{dl} = \varepsilon_0 \varepsilon A/d \quad (4)$$

where ε is the dielectric constant of the environment, ε_0 is the vacuum permittivity, A is the electrode area and d is the thickness of the protective layer. As can be seen in Table 2 with increasing the graphene nanoparticle to the polymer structure, thickness increased and coating capacitance reduced. According to Table 2, it can be concluded that the protection efficiency increased when coating thickness increased. On the other hand, these results show

Table 1
Electrochemical parameters of electropolymerized of polyaniline and PANI/G nanocomposite coatings on Cu in aqueous 5000 ppm NaCl solution.

Sample	I_{corr} (μA cm^{-2})	E_{corr} (V vs.Ag/AgCl)	b_a (V/dec)	b_c (V/dec)	R_p (Ω cm^2)	CR (mm year^{-1})	P%	PE%
Blank	5.2	−0.283	0.274	0.036	2.8×10^3	2.00×10^{-2}	–	–
PANI	1.8	−0.030	0.079	0.081	1.06×10^4	4.00×10^{-3}	3.1	65.4
PANI/G	0.1	−0.234	0.027	0.017	1.5×10^5	9.00×10^{-5}	1.3	98.0

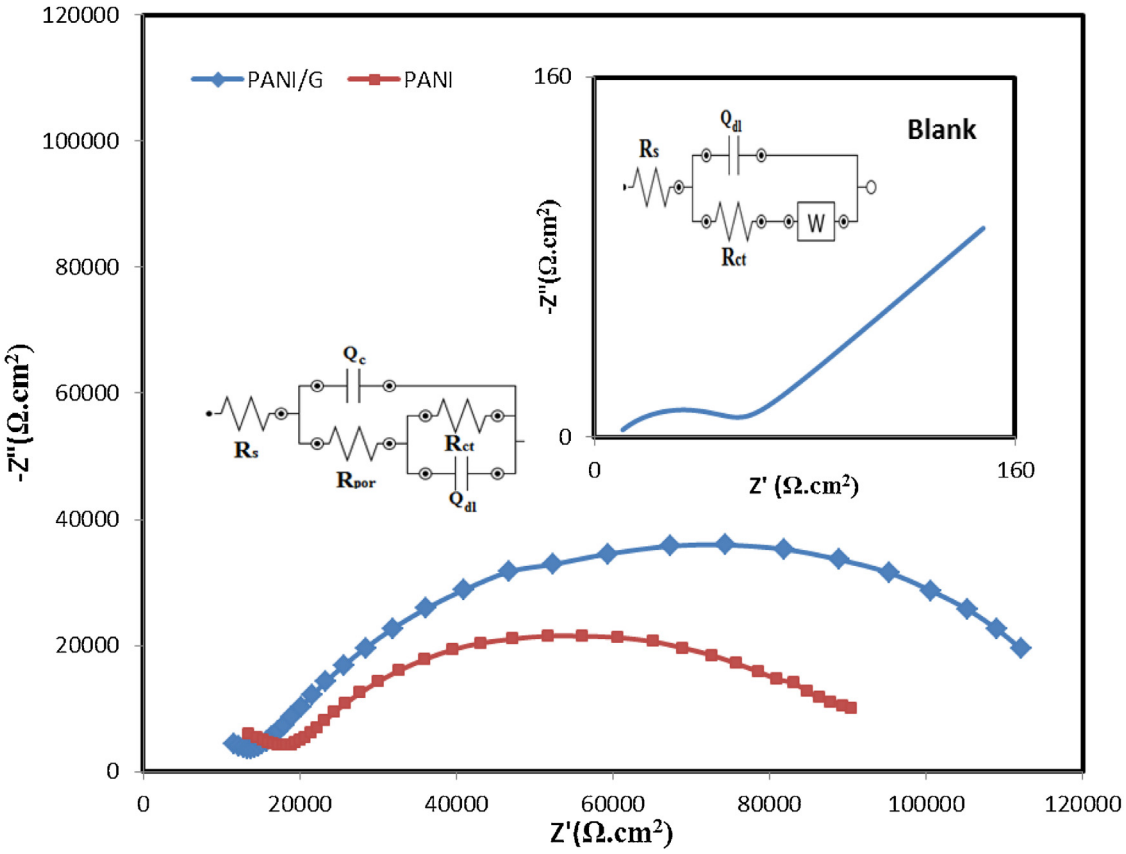

Fig. 9. Nyquist impedance plots for uncoated Cu and PANI/G nanocomposite coated Cu.

that the barrier properties of the coating on the Cu surface increased by graphene.

In fact, polyaniline is able to passivate steel surface and graphene improves barrier properties of the polymer coating considerably. As it was discussed above, Flaky shaped nanostructured of PANI/G nanocomposite may develop barrier properties of the PANI/G nanocomposite coatings systems. On the other hand, oxidation of Cu atoms to Cu^{+2} ions on the pinhole areas and defects causes the primary shift to the active potentials. Then polyaniline may be converted from emeraldine salt (ES) to leucoemeraldine base (LB) in the polymeric coating. By reduction of polyaniline-emeraldine salt (ES) to leucoemeraldine base (LB), the sulfate anions which are available as dopants in the conductive polymer are released and become available at the interface of the substrate and polymeric coating that they would tend to react with Cu cations and form a passivating complex. The role of a polyaniline layer in corrosion inhibition can be described by the following mechanism [20,73]:

$$2Cu + 3EM^{2+} + 3H_2O \rightarrow Cu_2O + 3LE + 6H^+$$

$$1/2O_2 + LE + H_2O \rightarrow EM^{2+} + 2OH^-$$

3.4. SEM characterization

The SEM images of abraded Cu electrode (image a), Cu electrode after corrosion (image b), PANI/G nanocomposite coated Cu electrode (image c) and PANI/G nanocomposite coated Cu electrode after corrosion (image d) are shown in Fig. 10. Image b shows that numerous large pits and inequalities were formed after corrosion, which reveals severe damage on the surface due to metal dissolution. Image c (PANI/G nanocomposite coating grown

Table 2
Impedance parameter values of the electrosynthesized polyaniline and PANI/G nanocomposite extracted from the fit to the equivalent circuit for the impedance spectra recorded in aqueous 5000 ppm NaCl solution.

Sample	R_s ($\Omega\,cm^2$)	R_{ct} ($k\Omega\,cm^2$)	R_{por} ($\Omega\,cm^2$)	Q_{dl} ($\Omega^{-1}\,cm^{-2}\,s^n$)	n	Q_c ($\Omega^{-1}\,cm^{-2}\,s^n$)	n	d[a] (μm)	PE%
PANI	20	90	600	450	0.6	350	0.55	0.1	63.3
PANI/G	22	118	623	125	0.8	180	0.75	0.4	72.0

Sample	R_s	R_{ct}	Q_{dl}	n	W
	12.5	33	3.5	0.4	0.023

[a] ($\varepsilon_0 = 8.85 \times 10^{-12}\,F\,cm^{-1}$, $\varepsilon = 5.9$, $A = 1\,cm^2$).

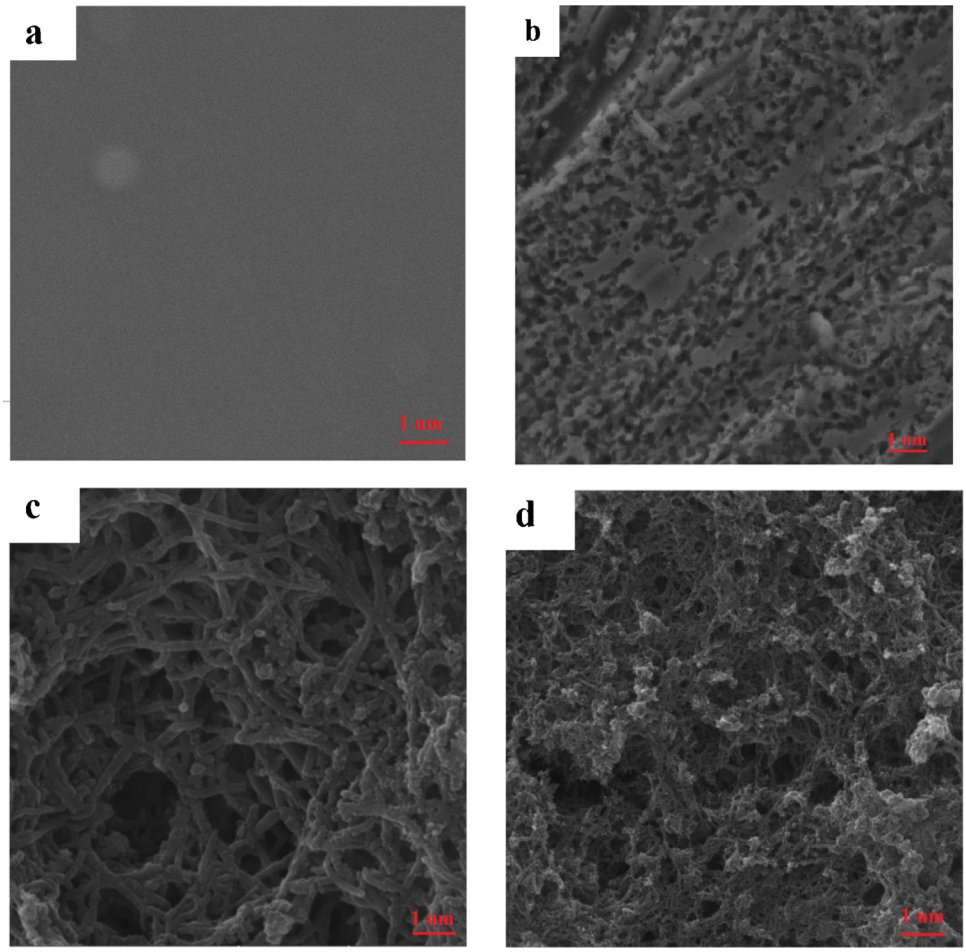

Fig. 10. SEM micrographs of abraded Cu (image a) pre-treated Cu after corrosion (image b), PANI/G nanocomposite coating (image c) and PANI/G nanocomposite coating after corrosion (image d).

by cyclic voltammetry) shows that the nanocomposite coating was electrodeposited on the electrode surface and protected it from the corrosion, and image d shows that the nanocomposite coating protects the Cu, which does not change dramatically. It clearly reveals that the formed coatings on the Cu surface are uniform and dense. The quality of the coatings is so excellent that no crack or detachment of the coatings is observed after the corrosion test.

4. Conclusion

Our study focused on the formation of PANI/G nanocomposite coatings as a means of corrosion protection of Cu. PANI/G nanocomposite coatings were successfully electrodeposited on Cu by cyclic voltammetry technique in a sulfuric acid medium and were then characterized by FTIR, UV–vis, XRD, and TGA. The coatings effectiveness against corrosion was tested by potentiodynamic polarization and EIS studies. PANI/G nanocomposite coatings were found to be capable of suggesting a noticeable enhancement of protection against Cu corrosion process carried out in 5000 ppm NaCl and the degradation rate decreased. The morphology of the composite film deposits was examined by SEM analysis to support the results obtained from EIS studies. SEM study on PANI/G nanocomposite coated Cu revealed that graphene nanoparticles were uniformly covered by polyaniline with a probable decrease in the number of polymer pores, and the morphology of PANI/G nanocomposite remained integrated and defect-free after immersion in 5000 ppm NaCl solution for 120 min. The coatings prepared from PANI/G nanocomposite were found to exhibit excellent corrosion resistance in aggressive environments. Thus, the use of polyaniline and graphene nanoparticles as a composite material increased significantly the anticorrosion performance of the substrate. The results showed that the use of polyaniline with graphene nanoparticles contributed to the formation of a composite layer, therefore shifting the corrosion potential of the metal substrate to lower values and decreasing the corrosion rate.

Acknowledgement

The authors are grateful to the University of Kashan for supporting this work by Grant No. 159194.

References

[1] B. Duran, G.z. Bereket, Cyclic voltammetric synthesis of poly(*N*-methyl pyrrole) on copper and effects of polymerization parameters on corrosion performance, Ind. Eng. Chem. Res. 51 (2012) 5246–5255.
[2] L. Nunez, E. Reguera, F. Corvo, E. Gonzalez, C. Vazquez, Corrosion of copper in seawater and its aerosols in a tropical island, Corros. Sci. 47 (2005) 461–484.
[3] B.M. Thethwayo, A.M. Garbers-Craig, Laboratory scale investigation into the corrosion of copper in a sulphur-containing environment, Corros. Sci. 53 (2011) 3068–3074.
[4] K. Khaled, Corrosion control of copper in nitric acid solutions using some amino acids—a combined experimental and theoretical study, Corros. Sci. 52 (2010) 3225–3234.
[5] K.-C. Chang, S.-T. Chen, H.-F. Lin, C.-Y. Lin, H.-H. Huang, J.-M. Yeh, Y.-H. Yu, Effect of clay on the corrosion protection efficiency of PMMA/Na+-MMT clay nanocomposite coatings evaluated by electrochemical measurements, Eur. Polym. J. 44 (2008) 13–23.

[6] V.J. Gelling, M.M. Wiest, D.E. Tallman, G.P. Bierwagen, G.G. Wallace, Electroactive-conducting polymers for corrosion control: 4. Studies of poly(3-octyl pyrrole) and poly(3-octadecyl pyrrole) on aluminum 2024-T3 alloy, Prog. Org. Coat. 43 (2001) 149–157.
[7] H.N.T. Le, B. Garcia, C. Deslouis, Q. Le Xuan, Corrosion protection and conducting polymers: polypyrrole films on iron, Electrochim. Acta 46 (2001) 4259–4272.
[8] K. Shah, J. Iroh, Electrochemical synthesis and corrosion behavior of poly(*N*-ethyl aniline) coatings on Al-2024 alloy, Synth. Met. 132 (2002) 35–41.
[9] N.J.F.W.W. Zeno, P.S. Peter, A.W. Douglas, Organic Coatings Science and Technology, John Wiley and Sons Publication, 2007.
[10] A. Skotheim, Handbook of Conducting Polymers, Marcel Dekker, New York, 1987.
[11] D.W. DeBerry, Modification of the electrochemical and corrosion behavior of stainless steels with an electroactive coating, J. Electrochem. Soc. 132 (1985) 1022–1026.
[12] J.C. Chiang, A.G. MacDiarmid, 'Polyaniline': protonic acid doping of the emeraldine form to the metallic regime, Synth. Met. 13 (1986) 193–205.
[13] B. Wessling, Dispersion as the link between basic research and commercial applications of conductive polymers (polyaniline), Synth. Met. 93 (1998) 143–154.
[14] I. Sekine, K. Kohara, T. Sugiyama, M. Yuasa, Syntheses of polymerized films on mild steels by electro-oxidation and electroreduction and their corrosion resistance, J. Electrochem. Soc. 139 (1992) 3090–3097.
[15] H. Hammache, L. Makhloufi, B. Saidani, Corrosion protection of iron by polypyrrole modified by copper using the cementation process, Corros. Sci. 45 (2003) 2031–2042.
[16] E. Kang, K. Neoh, K. Tan, Polyaniline: a polymer with many interesting intrinsic redox states, Prog. Polym. Sci. 23 (1998) 277–324.
[17] J. Prokeš, J. Stejskal, Polyaniline prepared in the presence of various acids: 2. Thermal stability of conductivity, Polym. Degrad. Stab. 86 (2004) 187–195.
[18] G. Gupta, N. Birbilis, A. Cook, A. Khanna, Polyaniline-lignosulfonate/epoxy coating for corrosion protection of AA2024-T3, Corros. Sci. 67 (2013) 256–267.
[19] M.M. Gvozdenović, B.N. Grgur, Electrochemical polymerization and initial corrosion properties of polyaniline-benzoate film on aluminum, Prog. Org. Coat. 65 (2009) 401–404.
[20] B. Wessling, Scientific and commercial breakthrough for organic metals, Synth. Met. 85 (1997) 1313–1318.
[21] S.R. Moraes, D. Huerta-Vilca, A.J. Motheo, Corrosion protection of stainless steel by polyaniline electrosynthesized from phosphate buffer solutions, Prog. Org. Coat. 48 (2003) 28–33.
[22] L. Zhong, S. Xiao, J. Hu, H. Zhu, F. Gan, Application of polyaniline to galvanic anodic protection on stainless steel in H_2SO_4 solutions, Corros. Sci. 48 (2006) 3960–3968.
[23] S. Sathiyanarayanan, S.S. Azim, G. Venkatachari, Corrosion protection of galvanized iron by polyaniline containing wash primer coating, Prog. Org. Coat. 65 (2009) 152–157.
[24] T. Schauer, A. Joos, L. Dulog, C. Eisenbach, Protection of iron against corrosion with polyaniline primers, Prog. Org. Coat. 33 (1998) 20–27.
[25] A.T. Özyılmaz, T. Tüken, B. Yazıcı, M. Erbil, The electrochemical synthesis and corrosion performance of polyaniline on copper, Prog. Org. Coat. 52 (2005) 92–97.
[26] G. Williams, R. Holness, D. Worsley, H. McMurray, Inhibition of corrosion-driven organic coating delamination on zinc by polyaniline, Electrochem. Commun. 6 (2004) 549–555.
[27] Y. Zhang, Y. Shao, T. Zhang, G. Meng, F. Wang, High corrosion protection of a polyaniline/organophilic montmorillonite coating for magnesium alloys, Prog. Org. Coat. 76 (2013) 804–811.
[28] M. Mahmoudian, Y. Alias, W. Basirun, M. Ebadi, Effects of different polypyrrole/TiO_2 nanocomposite morphologies in polyvinyl butyral coatings for preventing the corrosion of mild steel, Appl. Surf. Sci. 268 (2013) 302–311.
[29] S. Abaci, B. Nessark, Characterization and corrosion protection properties of composite material (PANI + TiO_2) coatings on A304 stainless steel, J. Coat. Technol. Res. 12 (2015) 107–120.
[30] Y. Jafari, M. Shabani-Nooshabadi, S.M. Ghoreishi, Electropolymerized coatings of poly(*o*-anisidine) and poly(*o*-anisidine)-TiO_2 nanocomposite on aluminum alloy 3004 by using the galvanostatic method and their corrosion protection performance, Polym. Adv. Technol. 25 (2014) 279–287.
[31] C.J. Weng, Y.L. Chen, Y.S. Jhuo, L. Yi-Li, J.M. Yeh, Advanced antistatic/anticorrosion coatings prepared from polystyrene composites incorporating dodecylbenzenesulfonic acid-doped SiO_2@ polyaniline core–shell microspheres, Polym. Int. 62 (2013) 774–782.
[32] A. Mostafaei, F. Nasirpouri, Epoxy/polyaniline–ZnO nanorods hybrid nanocomposite coatings: synthesis, characterization and corrosion protection performance of conducting paints, Prog. Org. Coat. 77 (2014) 146–159.
[33] M. Palimi, M. Rostami, M. Mahdavian, B. Ramezanzadeh, A study on the corrosion inhibition properties of silane-modified Fe_2O_3 nanoparticle on mild steel and its effect on the anticorrosion properties of the polyurethane coating, J. Coat. Technol. Res. 12 (2015) 277–292.
[34] A.M. Kumar, Z.M. Gasem, Effect of functionalization of carbon nanotubes on mechanical and electrochemical behavior of polyaniline nanocomposite coatings, Surf. Coat. Technol. 276 (2015) 416–423.
[35] P. Deshpande, S. Vathare, S. Vagge, E. Tomšík, J. Stejskal, Conducting polyaniline/multi-wall carbon nanotubes composite paints on low carbon steel for corrosion protection: electrochemical investigations, Chem. Pap. 67 (2013) 1072–1078.
[36] B.P. Singh, B.K. Jena, S. Bhattacharjee, L. Besra, Development of oxidation and corrosion resistance hydrophobic graphene oxide-polymer composite coating on copper, Surf. Coat. Technol. 232 (2013) 475–481.
[37] K. Novoselov, D. Jiang, F. Schedin, T. Booth, V. Khotkevich, S. Morozov, A. Geim, Two-dimensional atomic crystals, Proc. Natl. Acad. Sci. U. S. A. 102 (2005) 10451–10453.
[38] K.S. Novoselov, A.K. Geim, S. Morozov, D. Jiang, Y. Zhang, S.A. Dubonos, I. Grigorieva, A. Firsov, Electric field effect in atomically thin carbon films, Science 306 (2004) 666–669.
[39] M. Zhou, Y. Zhai, S. Dong, Electrochemical sensing and biosensing platform based on chemically reduced graphene oxide, Anal. Chem. 81 (2009) 5603–5613.
[40] C. Shan, H. Yang, J. Song, D. Han, A. Ivaska, L. Niu, Direct electrochemistry of glucose oxidase and biosensing for glucose based on graphene, Anal. Chem. 81 (2009) 2378–2382.
[41] Y. Sui, J. Appenzeller, Screening and interlayer coupling in multilayer graphene field-effect transistors, Nano Lett. 9 (2009) 2973–2977.
[42] Y. Wang, Z. Shi, Y. Huang, Y. Ma, C. Wang, M. Chen, Y. Chen, Supercapacitor devices based on graphene materials, J. Phys. Chem. C 113 (2009) 13103–13107.
[43] Y. Jin, M. Fang, M. Jia, In situ one-pot synthesis of graphene–polyaniline nanofiber composite for high-performance electrochemical capacitors, Appl. Surf. Sci. 308 (2014) 333–340.
[44] W. Choi, I. Lahiri, R. Seelaboyina, Y.S. Kang, Synthesis of graphene and its applications: a review, Crit. Rev. Solid State Mater. Sci. 35 (2010).
[45] D.R. Cooper, B. D'Anjou, N. Ghattamaneni, B. Harack, M. Hilke, A. Horth, N. Majlis, M. Massicotte, L. Vandsburger, E. Whiteway, Experimental review of graphene, ISRN Condens. Matter Phys. 2012 (2012).
[46] C.H. Chang, T.C. Huang, C.W. Peng, T.C. Yeh, H.I. Lu, W.I. Hung, C.J. Weng, T.I. Yang, J.M. Yeh, Novel anticorrosion coatings prepared from polyaniline/graphene composites, Carbon 50 (2012) 5044–5051.
[47] Y.H. Yu, Y.Y. Lin, C.H. Lin, C.C. Chan, Y.C. Huang, High-performance polystyrene/graphene-based nanocomposites with excellent anti-corrosion properties, Polym. Chem. 5 (2014) 535–550.
[48] B.P. Singh, S. Nayak, K.K. Nanda, B.K. Jena, S. Bhattacharjee, L. Besra, The production of a corrosion resistant graphene reinforced composite coating on copper by electrophoretic deposition, Carbon 61 (2013) 47–56.
[49] O.C. Compton, S. Kim, C. Pierre, J.M. Torkelson, S.T. Nguyen, Crumpled graphene nanosheets as highly effective barrier property enhancers, Adv. Mater. 22 (2010) 4759–4763.
[50] M. Shabani-Nooshabadi, M. Mollahoseiny, Y. Jafari, Electropolymerized coatings of polyaniline on copper by using the galvanostatic method and their corrosion protection performance in HCl medium, Surf. Interface Anal. 46 (2014) 472–479.
[51] A.M. Fenelon, C.B. Breslin, Polyaniline-coated iron: studies on the dissolution and electrochemical activity as a function of pH, Surf. Coat. Technol. 190 (2005) 264–270.
[52] B. Gupta, A.K. Singh, R. Prakash, Electrolyte effects on various properties of polycarbazole, Thin Solid Films 519 (2010) 1016–1019.
[53] T. Tüken, B. Yazıcı, M. Erbil, Polypyrrole/polythiophene coating for copper protection, Prog. Org. Coat. 53 (2005) 38–45.
[54] F. Branzoi, V. Branzoi, Z. Pahom, Monolayer and bilayer conducting polymer coatings for corrosion protection of copper in 0.5 M H_2SO_4 solutions, Rev. Roum. Chim. 58 (2013) 49–58.
[55] M. Kraljić, Z. Mandić, L. Duić, Inhibition of steel corrosion by polyaniline coatings, Corros. Sci. 45 (2003) 181–198.
[56] G. de T Andrade, M.a.J. Aguirre, S.R. Biaggio, Influence of the first potential scan on the morphology and electrical properties of potentiodynamically grown polyaniline films, Electrochim. Acta 44 (1998) 633–642.
[57] X.M. Feng, R.M. Li, Y.W. Ma, R.F. Chen, N.E. Shi, Q.L. Fan, W. Huang, One-step electrochemical synthesis of graphene/polyaniline composite film and its applications, Adv. Funct. Mater. 21 (2011) 2989–2996.
[58] A.M. Kumar, Z.M. Gasem, In situ electrochemical synthesis of polyaniline/f-MWCNT nanocomposite coatings on mild steel for corrosion protection in 3.5% NaCl solution, Prog. Org. Coat. 78 (2015) 387–394.
[59] A. Eftekhari, P. Jafarkhani, Polymerization of aniline through simultaneous chemical and electrochemical routes, Polym. J. 38 (2006) 651–658.
[60] X. Feng, G. Yang, Q. Xu, W. Hou, J.J. Zhu, Self-assembly of polyaniline/Au composites: from nanotubes to nanofibers, Macromol. Rapid Commun. 27 (2006) 31–36.
[61] S. Park, J. An, I. Jung, R.D. Piner, S.J. An, X. Li, A. Velamakanni, R.S. Ruoff, Colloidal suspensions of highly reduced graphene oxide in a wide variety of organic solvents, Nano Lett. 9 (2009) 1593–1597.
[62] D. Li, M.B. Mueller, S. Gilje, R.B. Kaner, G.G. Wallace, Processable aqueous dispersions of graphene nanosheets, Nat. Nanotechnol. 3 (2008) 101–105.
[63] D. Gui, C. Liu, F. Chen, J. Liu, Preparation of polyaniline/graphene oxide nanocomposite for the application of supercapacitor, Appl. Surf. Sci. 307 (2014) 172–177.
[64] A. Oyefusi, O. Olanipekun, G.M. Neelgund, D. Peterson, J.M. Stone, E. Williams, L. Carson, G. Regisford, A. Oki, Hydroxyapatite grafted carbon nanotubes and graphene nanosheets: promising bone implant materials, Spectrochim. Acta, Part A 132 (2014) 410–416.

[65] S. Ran, C. Chen, Z. Guo, Z. Fang, Char barrier effect of graphene nanoplatelets on the flame retardancy and thermal stability of high-density polyethylene flame-retarded by brominated polystyrene, J. Appl. Polym. Sci. 131 (2014).
[66] S. Chaudhari, S. Sainkar, P. Patil, Anticorrosive properties of electrosynthesized poly(*o*-anisidine) coatings on copper from aqueous salicylate medium, J. Phys. D: Appl. Phys. 40 (2007) 520.
[67] C. Oueiny, S. Berlioz, F.-X. Perrin, Carbon nanotube–polyaniline composites, Prog. Polym. Sci. 39 (2014) 707–748.
[68] M. Shabani-Nooshabadi, S.M. Ghoreishi, M. Behpour, Direct electrosynthesis of polyaniline–montmorrilonite nanocomposite coatings on aluminum alloy 3004 and their corrosion protection performance, Corros. Sci. 53 (2011) 3035–3042.
[69] W. Araujo, I. Margarit, M. Ferreira, O. Mattos, P.L. Neto, Undoped polyaniline anticorrosive properties, Electrochim. Acta 46 (2001) 1307–1312.
[70] M. Shabani-Nooshabadi, M. Ghandchi, Santolina chamaecyparissus extract as a natural source inhibitor for 304 stainless steel corrosion in 3.5% NaCl, J. Ind. Eng. Chem. 31 (2015) 231–237.
[71] M. Behpour, S.M. Ghoreishi, N. Mohammadi, N. Soltani, M. Salavati-Niasari, Investigation of some Schiff base compounds containing disulfide bond as HCl corrosion inhibitors for mild steel, Corros. Sci. 52 (2010) 4046–4057.
[72] S.M. Ghoreishi, M. Shabani-Nooshabadi, M. Behpour, Y. Jafari, Electrochemical synthesis of poly(*o*-anisidine) and its corrosion studies as a coating on aluminum alloy 3105, Prog. Org. Coat. 74 (2012) 502–510.
[73] M. Nicho, H. Hu, J. González-Rodriguez, V. Salinas-Bravo, Protection of stainless steel by polyaniline films against corrosion in aqueous environments, J. Appl. Electrochem. 36 (2006) 153–160.